



# 海洋地质与第四纪地质

MARINE GEOLOGY & QUATERNARY GEOLOGY

## 晚中新世柴达木盆地低偏心率时期倾角驱动的干湿变化

邓欣宜, 聂军胜, 任雪萍

### Obliquity-driven moisture changes in Qaidam Basin in Late Miocene during low eccentricity period

DENG Xinyi, NIE Junsheng, and REN Xueping

在线阅读 View online: <https://doi.org/10.16562/j.cnki.0256-1492.2022052601>

## 您可能感兴趣的其他文章

### Articles you may be interested in

#### 珠江口内伶仃洋晚第四纪黏土矿物组成特征及对源区气候变化的指示

Late Quaternary clay minerals in the inner Lingdingyang of the Pearl River Estuary, southern China: Implications for paleoclimate changes at the provenance

海洋地质与第四纪地质. 2021, 41(5): 202

#### 渤海湾西岸晚更新世以来的沉积环境演化及碳埋藏评价

Environmental evolution and carbon burial assessment of the west coast of Bohai Bay since Late Pleistocene

海洋地质与第四纪地质. 2021, 41(6): 194

#### 江苏中部海岸晚第四纪沉积物的粒度与磁化率特征及其古环境意义

Characteristics of grain size and magnetic susceptibility of the Late Quaternary sediments from core 07SR01 in the middle Jiangsu coast and their paleoenvironmental significances

海洋地质与第四纪地质. 2021, 41(5): 210

#### 南薇西含油气盆地地层层序及生储盖组合特征

Characteristics of stratigraphic sequence and the source-reservoir-cap assemblages in the Nanweixi petroliferous basin

海洋地质与第四纪地质. 2021, 41(6): 163

#### 北康盆地基底卷入断层特征及其对南海南部构造演化的启示

Features of the basement-involved faults in the Beikang Basin and their implications for the tectonic evolution of the southern South China Sea

海洋地质与第四纪地质. 2021, 41(4): 116

#### 南黄海中部隆起晚新近纪—第四纪沉积序列的地层划分与沉积演化

Stratigraphic classification and sedimentary evolution of the late Neogene to Quaternary sequence on the Central Uplift of the South Yellow Sea

海洋地质与第四纪地质. 2021, 41(5): 25



关注微信公众号，获得更多资讯信息

邓欣宜, 聂军胜, 任雪萍. 晚中新世柴达木盆地低偏心率时期倾角驱动的干湿变化 [J]. 海洋地质与第四纪地质, 2022, 42(6): 193-199.  
DENG Xinyi, NIE Junsheng, REN Xueping. Obliquity-driven moisture changes in Qaidam Basin in Late Miocene during low eccentricity period[J]. Marine Geology & Quaternary Geology, 2022, 42(6): 193-199.

# 晚中新世柴达木盆地低偏心率时期倾角驱动的干湿变化

邓欣宜, 聂军胜, 任雪萍

兰州大学资源环境学院, 西部环境教育部重点实验室, 兰州 730000

**摘要:** 当前间冰期正处在地球轨道低偏心率时期, 在全球变暖的大趋势下北半球冰盖正逐渐消融。因此, 解析北半球无冰背景下低偏心率时期亚洲内陆干湿变化规律和驱动机制, 对预测该地区未来环境变化具有重要意义。然而, 以前的研究关注亚洲内陆低偏心率时期环境变化的高分辨率记录较少, 限制了对该区干湿循环和驱动机制的理解。柴达木盆地位于东亚季风降水边缘, 对干湿变化非常敏感。选取柴达木盆地东北部大红沟剖面河湖相沉积地层, 利用频率磁化率指标重建晚中新世时期 (9~12 Ma) 高分辨率干湿变化历史, 揭示了典型的低偏心率时期干湿变化主导周期和轨道斜率驱动机制。结果表明, 在低偏心率时期 (9.2~9.4、9.6~9.8 和 11.2~11.4 Ma), 该区域干湿变化以 4 万年周期为主, 对应倾角变化, 说明在岁差振幅较小时, 倾角变化可能上升为轨道调控干旱区干湿变化的主导因素。这一发现对理解未来气候变化具有一定的借鉴意义。

**关键词:** 低偏心率; 干湿变化; 周期分析; 轨道驱动; 柴达木盆地

中图分类号:P532 文献标识码:A DOI: 10.16562/j.cnki.0256-1492.2022052601

## Obliquity-driven moisture changes in Qaidam Basin in Late Miocene during low eccentricity period

DENG Xinyi, NIE Junsheng, REN Xueping

Key Laboratory of West China's Environmental System, Ministry of Education, College of Earth Environmental Science, Lanzhou University, Lanzhou 730000, China

**Abstract:** The present interglacial period is at a period of low eccentricity, and the ice sheets in the northern hemisphere are gradually melting due to the global warming. Understanding the variation and the mechanism of dry-wet alternation in Asian inland during low eccentricity period under the ice-free background of the northern hemisphere is very important to predict the future environmental changes in the area. At present, little attention is paid to high-resolution records of environment variations during low eccentricity periods in inland Asia, which limits the understanding of moisture changes and the mechanism in the region. The Qaidam Basin, located at the edge of East Asian monsoon rain zone, is very sensitive to dry-wet climate alternation. In this study, we selected the fluvial-lacustrine strata of the Dahonggou section in the northeastern Qaidam Basin, along which the frequency magnetic susceptibility was measured, to reconstruct the high-resolution moisture history of the Late Miocene (12~9 Ma). Results revealed typical dry-wet changes and show that the local climate change has a clear 40-ka cycle, corresponding to the obliquity in typical low eccentricity condition when the precession amplitude is small during 9.4~9.2 Ma, 9.8~9.6 Ma, and 11.4~11.2 Ma. It suggests that obliquity factor may rise and become a dominant factor on orbital regulation of environment in arid area. This finding has important implications for understanding future climate change.

**Key words:** low eccentricity; moisture changes; cycle analysis; orbital forcing; Qaidam Basin

人类目前生活的地质时期是 1.17 万年至今的全新世, 这是一个地球轨道偏心率较低、太阳辐射振幅变化较小的间冰期<sup>[1-2]</sup>。在工业化革命后温室气体持续增排的背景下, 到 21 世纪末大气 CO<sub>2</sub> 浓度可能上升到 (500~600) × 10<sup>-6</sup><sup>[3]</sup>, 远高于北半球冰

盖形成时的阈值。未来全球气候可能会继续变暖, 演变成北半球夏季无冰的“单极冰室模式”<sup>[4-5]</sup>。晚中新世是一个距今较近的温暖期, 该时期仅在南极形成了大规模冰盖, 北半球尚未形成大规模的稳定冰盖<sup>[6-7]</sup>。因此, 分析过去暖期的干湿变化, 如晚中

资助项目: 科技部第二次青藏高原综合科学考察研究专题项目“碰撞以来古地理格局与构造地貌过程”(2019QZKK0704)

作者简介: 邓欣宜(2000—), 男, 硕士研究生, 自然地理学专业, E-mail: dengxy18@lzu.edu.cn

收稿日期: 2022-05-26; 改回日期: 2022-07-09. 文凤英编辑

新世的低偏心率期气候干湿变化规律及其对地球轨道参数的响应机制, 对预测未来亚洲地区气候干湿变化具有重要参考价值<sup>[8-16]</sup>。

近几十年来, 国内外许多学者基于中国黄土<sup>[17-25]</sup>、石笋<sup>[26-27]</sup>、湖泊<sup>[24, 28-29]</sup>、海洋沉积物<sup>[30-33]</sup>等载体, 对与当前天文背景(低偏心率下的全新世)相似的温暖间冰期, 如深海氧同位素 11 和 19 阶段(MIS 11 和 MIS 19)等, 开展了广泛的研究, 为剖析区域和全球气候演化的驱动机制奠定了重要基础。以 MIS11 为例<sup>[34]</sup>, 东亚高分辨率石笋氧同位素记录的轨道尺度降水变化具有明显的 2 万年周期, 支持了北半球夏季太阳辐射对亚洲夏季风降水的控制<sup>[26-27]</sup>, 而中国黄土磁化率记录的降水变化存在显著 10 万年周期, 这与北半球冰量的周期性变化一致<sup>[14, 35-37]</sup>。此外, 模拟结果表明, 在低偏心率时期, 倾角变化是控制气候变化的主要因素。例如, Wu 等<sup>[38]</sup>利用大气、生物、海洋和海冰地球系统模型(LOVECLIM)模拟了南北两个半球海温和海冰在 417~511 ka 期间对岁差和倾角的不同响应, 发现低偏心率时期(417~460 ka)倾角变化发挥主导作用。同时, 第四纪约 1~2 Ma 时期大气环流模型(GCM)的结果也表明, 低偏心率时期倾角变化控制着南北半球高纬度冰量和气候变化<sup>[39]</sup>。上述研究主要集中在北半球有冰时期, 北半球没有永久冰盖时低偏心率时期气候变化研究还很薄弱, 气候变化如何响应轨道参数变化的机制尚不清楚, 这些都限制了对亚洲内陆环境未来变化的预测<sup>[40]</sup>。

以往对中国北方干旱-半干旱地区高分辨率气候变化的研究偏重从较长尺度理解轨道尺度气候干湿变化规律, 少有针对低偏心率这一特殊短时期轨道尺度干湿变化规律和驱动机制研究<sup>[41-43]</sup>, 制约了对干旱区低偏心率时期轨道尺度干湿变化规律和驱动机制的认识。例如, 在柴达木盆地、贵德盆地、天水盆地、兰州盆地基于磁化率或 Rb/Sr 重建的古气候变化记录共同表明, 晚渐新世(28.1~24.1 Ma)、早中新世(21.5~17.2 Ma)和晚中新世(约 14~7 Ma)降水变化以显著的 10 万年周期为主, 这归因于偏心率调节的降水变化<sup>[11, 16, 41-43]</sup>。因此, 为解答亚洲干旱区低偏心率时期气候变化如何响应地球轨道参数, 亟需获取对气候变化更为敏感地区的高分辨率古气候记录。

柴达木盆地是重建低偏心率时期高分辨率轨道尺度气候变化历史的理想场所<sup>[42, 44]</sup>。首先, 柴达木盆地处于东亚季风区、亚洲内陆干旱区和青藏高原高寒区这三大自然区的交汇位置, 对气候变化尤

为敏感<sup>[45-46]</sup>。其次, 柴达木盆地内发育巨厚的新生代河湖相地层, 沉积速率高, 较完整地记录了气候变化的详细信息<sup>[47-50]</sup>; 位于其东北部的大红沟剖面地层出露较为连续, 晚中新世时段平均沉积速率高达约 34 cm/ka, 提供了高分辨率环境干湿变化研究的良好地质载体<sup>[51-52]</sup>。本研究选取柴达木盆地大红沟剖面河湖相沉积地层为研究对象, 运用频率磁化率指标, 重建北半球无冰的晚中新世(9~12 Ma)高分辨率干湿变化历史, 对比轨道参数, 探究在低偏心率时期该区干湿变化规律、主导周期及其对地球轨道参数的响应机制。

## 1 研究区概况

柴达木盆地是中国西北内陆地区、青藏高原东北部一个封闭的山间断陷盆地, 位于 35°~39°N、90°~99°E(图 1)。盆地被周围高大山系所环绕, 西北、东北和南部分别为阿尔金山、祁连山-南山和昆仑山系, 周围山脉海拔范围高达 4000~5000 m, 盆地内部海拔为 2700~3000 m。气候方面, 盆地当前大气环流模式主要受西风环流控制<sup>[53]</sup>, 而盆内以高寒大陆性气候为主, 终年干旱少雨, 多大风天气; 降水量相对较强(年均 2000~3000 mm)。构造上, 盆地被东北部祁连山逆冲断裂、西北部阿尔金走滑断裂、南部东昆仑断裂和东部鄂拉山走滑断裂 4 个典型断裂带包围, 在盆地的形成和演化中发挥着重要作用<sup>[54]</sup>。盆内部新生代河湖相地层分布广泛, 大量沉积物质主要由周边山地剥蚀和风化作用提供, 富含新生代环境演化过程的关键信息<sup>[47]</sup>。

大红沟剖面(37°31'N、95°09'E)位于柴达木盆地东北部, 出露较为连续, 全长 6 200 m(图 1)。剖面地层由老到新依次划分为路乐河、下干柴沟、上干柴沟、下油砂山、上油砂山和狮子沟组, 主要为河湖相沉积。其中, 本文研究的 9~12 Ma 段地层主要包括下干柴沟组(3 250~3 500 m)上部和上干柴沟组大部(3 500~4 400 m)。下干柴沟组以曲流河相沉积为主, 岩性包括砂岩、泥质粉砂岩夹杂砾岩等, 上干柴沟组则是以曲流河-滨湖相沉积为主, 岩性以棕红色泥岩和黄绿色砂岩为主<sup>[55]</sup>。

目前对于大红沟剖面地层古地磁年代还存在三种不同的年代模式, 第一种观点结合孢粉、介形虫、叶化石和介形虫等将剖面年代界定为古新世—晚中新世(约 52~7 Ma)<sup>[48, 50]</sup>; 第二种观点结合新发现的红沟动物化石群将该剖面年代界定为晚渐新

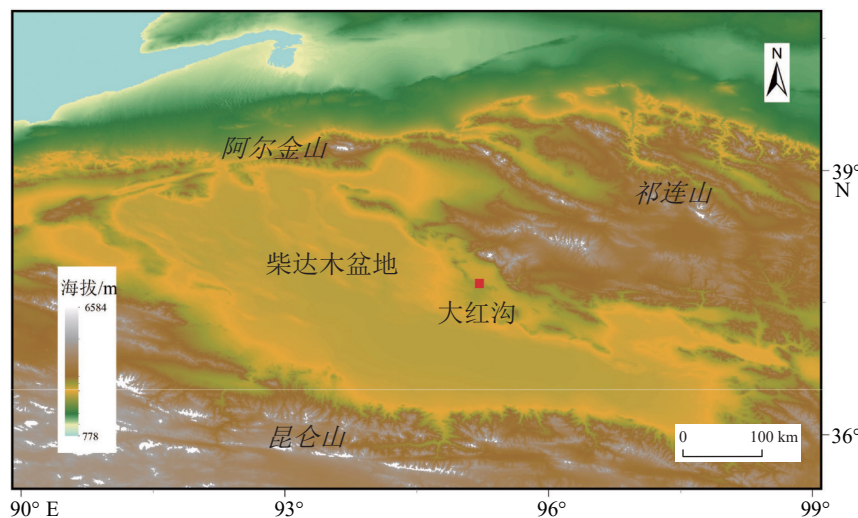


图 1 研究区及采样剖面位置图

Fig.1 The study area showing sampling section location

世—上新世(约 25~5 Ma), 与地层中发现的新近纪孢粉时代较为吻合<sup>[51]</sup>, 第三种观点则将地层年代界定为早中新世—上新世(约 21~5 Ma)<sup>[52]</sup>。其中, 后面两种年代模式都是结合晚中新世哺乳动物化石群得到, 年代主要差别在于路乐河组, 而其他时段古地磁极性柱对比较好, 说明剖面地层古地磁结果较为可靠<sup>[51-52]</sup>。此外, 在第三种年代模式下的古气候研究发现, 大红沟剖面降水在中中新世暖期增强, 与区域乃至全球气候变化较为一致, 也说明该年代模式是相对可靠的。因此本研究基于第三种年代模式进行高分辨率古气候重建。根据该年代模型已有的古地磁控制点<sup>[52]</sup>建立了 9~12 Ma 时期对应的时间标尺(4 个古地磁年代控制点对应年代分别是 12.049、11.056、9.786 和 9.105 Ma, 结合控制点线性内插可得到详细的年代序列), 为高分辨率轨道尺度干湿变化历史的重建提供了良好的年代基础<sup>[52]</sup>。

## 2 材料及方法

本剖面采样平均间隔 1 m, 共采集古环境样品 999 个, 样品平均时间分辨率为 3 ka。我们首先将散装样品在恒温烘箱(约 40℃)中烘干, 用研钵将样品研磨粉碎至无明显颗粒状(不破坏磁性矿物), 同时将粉末样品装入一个边长为 2 cm 的立方体(无磁性)塑料盒中压实固定并称重。然后, 在远离电磁场干扰的环境中测试每个样品的磁化率值。测试仪器采用 Barington MS2 磁化率仪, 分别获得低频(470 Hz)和高频(4700 Hz)磁化率( $\chi_{lf}$  和  $\chi_{hf}$ ), 并重复测量 2 次, 取其平均值。由平均高低频磁化率之

间的差值计算( $\chi_{fd} = \chi_{lf} - \chi_{hf}$ )可得频率磁化率( $\chi_{fd}$ )。频率磁化率通常反映超顺磁(SP)和单畴(SSD)临界点附近颗粒含量的变化<sup>[56]</sup>, 这些颗粒的形成主要受气候变化相关的成壤作用控制<sup>[57]</sup>。同时, 以往基于黄土高原现代表层土壤中  $\chi_{fd}$  与气候变化(降水和温度)关系的研究指出,  $\chi_{fd}$  代表成壤或风化过程产生的超顺磁颗粒中亚铁磁性矿物含量的变化, 与降水变化的相关性较高,  $\chi_{fd}$  越高表明降水相对越多<sup>[58-60]</sup>。

对于河湖相沉积物, 频率磁化率指标蕴含的信息更加复杂, 可能受到其他因素的影响, 比如沉积后的还原溶解作用及搬运过程中基岩碎屑物质加入的影响等。但是, 大红沟剖面晚中新世以河流相和边缘湖相沉积为主, 非封闭性湖泊, 还原作用相对弱, 磁性矿物发生溶解的可能性较小。另外, 该剖面热退磁方法揭示出该序列沉积物中的主要载磁性矿物包括磁铁矿和赤铁矿<sup>[52]</sup>。而 9~12 Ma 期间大红沟剖面物质来源相对稳定<sup>[52]</sup>, 说明碎屑物质来源变化不大, 加入到沉积物中的基岩碎屑物质没有明显变化, 不影响轨道周期的研究。因此我们认为在轨道尺度上, 其他因素引起的误差有限, 不足以影响对轨道周期变化的讨论。因此, 本研究采用大红沟剖面沉积序列中的  $\chi_{fd}$  记录来指代柴达木盆地东北部 9~12 Ma 的降水变化。

## 3 结果与讨论

将大红沟剖面频率磁化率  $\log_{10}\chi_{fd}$  曲线与同时期地球轨道参数对比(图 2), 结果表明, 在低偏心率和低进动(岁差)振幅时期(9.2~9.4、9.6~9.8、11.2~11.4 Ma), 大红沟剖面频率磁化率变化以明

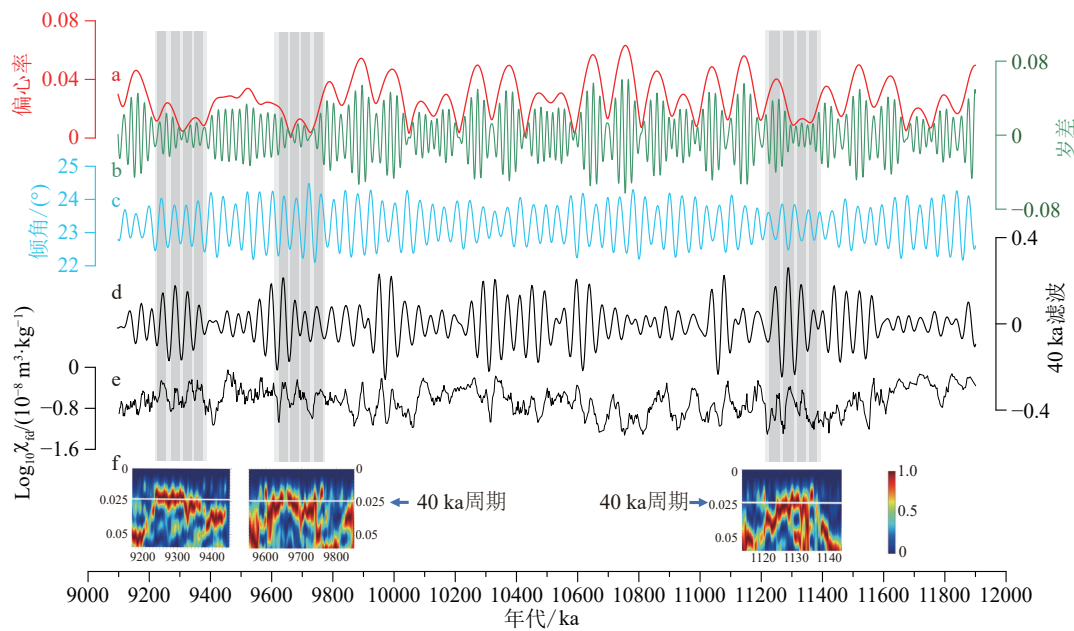


图 2 大红沟剖面 9~12 Ma 频率磁化率记录和地球轨道参数对比图

a—c. 地球轨道参数偏心率(红线)、岁差(绿线)和倾角(蓝线)曲线<sup>[2]</sup>, d. 频率磁化率( $\chi_{\text{fd}}$ )4 万年周期滤波曲线, e.  $\log_{10}\chi_{\text{fd}}$  曲线, f. 低偏心率时期频率磁化率小波分析图, 白线及箭头指示频率 0.025。

Fig.2 Comparison in frequency magnetic susceptibility ( $\chi_{\text{fd}}$ ) recorded from the Dahonggou section with astronomical orbital parameter during 9 to 12 Ma

a-c. The earth's orbital parameters of eccentricity (red line), precession (green line), and obliquity<sup>[2]</sup>; d. 40 ka Gaussian bandpass filtered output of  $\chi_{\text{fd}}$ ; e.  $\log_{10}\chi_{\text{fd}}$  curve; f. the wavelet transform of  $\chi_{\text{fd}}$  during the period of low eccentricity, white line and arrows point at the frequency of 0.025.

显的 4 万年周期为主, 与倾角周期一致。同时, 从相位关系上看, 柴达木盆地低偏心率期(9.2~9.4 Ma 和 9.6~9.8 Ma), 气候干湿变化与倾角变化具有相同的相位变化关系, 倾角较大时, 气候较湿润(图 2); 然而, 在另外一段低偏心率期(11.2~11.4 Ma), 气候变化与倾角变化大致处于反相位关系(图 2), 造成差异的原因可能是干湿变化序列没有经过年代调谐, 轨道尺度上年代控制存在一定误差。上述结果表明, 低偏心率下柴达木盆地干湿变化受倾角变化控制。

前人研究发现, 在晚中新世的低偏心率和低进动振幅时段, 全球冰量变化和其他西风区气候变化也响应 4 万年周期性波动, 与我们的结果一致, 支持倾角驱动。例如, 根据南海 ODP1146 钻孔中晚中新世底栖有孔虫  $\delta^{18}\text{O}$  的记录, 冰量变化在此时期(约 9.2~9.7 Ma)以约 4 万年周期主导<sup>[6, 61-62]</sup>。此外, 有学者基于磁性地层和旋回地层学在西班牙东北部的普拉多剖面晚中新世(9.1~10.3 Ma)边缘湖相地层的研究发现, 在偏心率最低值时(如 9.6~9.8 Ma, 约 9.2~9.4 Ma)的地层旋回厚度明显高于全剖面平均岩层厚度, 推测在进动振幅较小的时期, 倾角变化可能对气候变化起主导作用<sup>[10]</sup>。

以往的研究表明, 轨道参数倾角的周期性变化会影响南北半球太阳辐射的时空分布, 倾角可以通过调节太阳辐射的温度梯度来影响极地冰量、西风急流和海陆热差, 进一步控制亚洲气候变化<sup>[15, 63-65]</sup>。

在前人研究基础上, 结合柴达木盆地气候变化与倾角关系分析, 推测倾角可能通过控制太阳辐射影响低偏心率时期(9.2~9.8 Ma 和 9.6~9.8 Ma)大红沟剖面的干湿变化。主要原因如下: 首先, 倾角变化影响中纬度西风环流强度和西风位置, 从而调节亚洲气候变化。倾角越大, 夏季北半球径向太阳辐射和温度梯度越小, 西风环流越弱, 位置越偏北, 降水越少<sup>[15]</sup>。本研究中柴达木盆地气候较为湿润, 推测该区域受西风影响较小, 且西风减弱和北撤也可能增强亚洲季风环流, 使柴达木盆地气候比较湿润。其次, 倾角通过改变南半球经向温度梯度来影响南极海洋冰盖动力学, 进一步增强了全球气候对倾角驱动的敏感性<sup>[65]</sup>。南极冰盖的扩张可以通过增强跨赤道压力梯度和潜热释放来增强东亚夏季风<sup>[66]</sup>, 而柴达木盆地的高降水在 9.2~9.4 Ma 和 9.6~9.8 Ma 对应于高倾角, 不利于南极冰盖增长<sup>[67]</sup>, 因此推测南极冰盖对该地区降水变化的影响较小。第三, 模拟和地质记录表明, 倾角也可能通过

直接控制北方夏季太阳辐射梯度来改变海陆热力差, 再通过调节高纬大陆低压系统和低纬海洋高压系统之间的热力差异, 对亚洲季风气候产生影响。因此, 高倾角可对应东亚夏季风降水增强, 并对周边内陆地区产生持续影响<sup>[63, 68]</sup>。近期的研究也已经指出, 柴达木盆地在晚中新世构造和轨道尺度上可能受到东亚夏季风的影响<sup>[12, 69]</sup>。因此, 基于以上讨论, 我们推测在晚中新世低偏心率时期, 倾角通过调节太阳辐射梯度, 影响亚洲夏季风, 进而控制柴达木盆地轨道尺度的干湿变化。

需要指出的是, 本文对于干湿变化的推断主要是基于频率磁化率单一指标记录, 该指标可以指示沉积物中 20~30 nm 级磁性矿物的含量, 这些细颗粒磁性矿物的含量主要是通过风化成壤作用产生的。因此, 该指标在河湖相沉积物中比磁化率指标具有更加明确的环境干湿变化指示意义。然而在更大的构造尺度上该指标的变化还可能受到岩性变化和构造活动等其他因素的影响, 因此本文主要讨论轨道尺度的环境变化。尽管如此, 建议未来还应继续开展基于其他指标和不同尺度的干湿变化研究, 进一步检验本文初步结论的正确性。

## 4 结论

本研究以青藏高原东北部柴达木盆地大红沟剖面晚中新世(12~9 Ma)河湖相沉积地层为研究对象, 在已有的古地磁年代标尺基础上, 运用频率磁化率指标分析低偏心率时期柴达木盆地高分辨率干湿变化规律和主导周期, 并通过对比地球轨道参数记录, 探讨了该时期干湿变化与地球轨道参数变化之间的响应关系。

研究表明, 晚中新世低偏心率时期(9.2~9.4 Ma, 9.6~9.8 Ma 和 11.2~11.4 Ma)岁差(进动)振幅较小, 柴达木盆地干湿变化具有明显的 4 万年周期, 说明低偏心率时期该区域干湿变化可能主要受倾角控制。其中, 9.4~9.2 Ma 和 9.8~9.6 Ma 时段降水变化与倾角变化具有同相位关系, 而 11.2~11.4 Ma 时段降水变化和倾角变化具有反相位关系, 这可能受到年代误差影响。结合前人研究, 我们推测低偏心率时期的倾角变化可能通过调节太阳辐射梯度来影响柴达木盆地干湿变化。

## 参考文献 (References)

- [1] Berger A, Loutre M F. An exceptionally long interglacial ahead? [J]. *Science*, 2002, 297(5585): 1287-1288.
- [2] Laskar J, Robutel P, Joutel F et al. A long-term numerical solution for the insolation quantities of the Earth [J]. *Astronomy & Astrophysics*, 2004, 428(1): 261-285.
- [3] IPCC. Climate Change 2014: Synthesis Report. Contribution of Working Groups I, II and III to the Fifth Assessment Report of the Intergovernmental Panel on Climate Change [M]. Geneva: IPCC, 2014.
- [4] Deconto R M, Pollard D, Wilson P A et al. Thresholds for Cenozoic bipolar glaciation [J]. *Nature*, 2008, 455(7213): 652-656.
- [5] Wunderling N, Willeit M, Donges J F et al. Global warming due to loss of large ice masses and Arctic summer sea ice [J]. *Nature Communications*, 2020, 11(1): 5177.
- [6] Holbourn A E, Kuhnt W, Clemens S C et al. Late Miocene climate cooling and intensification of southeast Asian winter monsoon [J]. *Nature Communications*, 2018, 9(1): 1584.
- [7] Westerhold T, Marwan N, Drury A J et al. An astronomically dated record of Earth's climate and its predictability over the last 66 million years [J]. *Science*, 2020, 369(6509): 1383-1387.
- [8] 丁仲礼. 米兰科维奇冰期旋回理论: 挑战与机遇[J]. *第四纪研究*, 2006, 26(5): 710-717. [DING Zhongli. The milankovitch theory of Pleistocene glacial cycles: challenges and chances [J]. *Quaternary Sciences*, 2006, 26(5): 710-717.]
- [9] 汪品先. 全球季风的地质演变[J]. *科学通报*, 2009, 54(5): 535-556. [WANG Pinxian. Global monsoon in a geological perspective [J]. *Chinese Science Bulletin*, 2009, 54(5): 535-556.]
- [10] Abels H A, Aziz H A, Ventra D et al. Orbital climate forcing in mudflat to marginal Lacustrine deposits in the Miocene Teruel Basin (Northeast Spain) [J]. *Journal of Sedimentary Research*, 2009, 79(11): 831-847.
- [11] Ao H, Rohling E J, Zhang R et al. Global warming-induced Asian hydrological climate transition across the Miocene-Pliocene boundary [J]. *Nature Communications*, 2021, 12(1): 6935.
- [12] Gao P, Nie J S, Yan Q et al. Millennial resolution late Miocene Northern China precipitation record spanning astronomical analogue interval to the future [J]. *Geophysical Research Letters*, 2021, 48(15): e2021GL093942.
- [13] 杨彦峰, 符超峰, 徐新文, 等. 青藏高原东北缘尖扎盆地晚中新世地层绝对天文年代标尺的建立[J]. *地球科学与环境学报*, 2021, 43(4): 710-723. [YANG Yanfeng, FU Chaofeng, XU Xinwen et al. Establishment of absolute astronomical time scale of late Miocene strata in Jianzha Basin, the northeastern margin of Tibetan Plateau, China [J]. *Journal of Earth Sciences and Environment*, 2021, 43(4): 710-723.]
- [14] An Z S, Wu G X, Li J P et al. Global monsoon dynamics and climate change [J]. *Annual Review of Earth and Planetary Sciences*, 2015, 43: 29-77.
- [15] Frisch K, Voigt S, Verestek V et al. Long-period astronomical forcing of Westerlies' strength in central Asia during Miocene climate cooling [J]. *Paleoceanography and Paleoclimatology*, 2019, 34(11): 1784-1806.
- [16] Wang Y C, Lu H Y, Wang K X et al. Combined high- and low-latitude forcing of East Asian monsoon precipitation variability in the Pliocene

- warm period [J]. *Science Advances*, 2020, 6(46): eabc2414.
- [17] Wu N Q, Chen X Y, Rousseau D D et al. Climatic conditions recorded by terrestrial mollusc assemblages in the Chinese Loess Plateau during marine Oxygen Isotope Stages 12-10 [J]. *Quaternary Science Reviews*, 2007, 26(13-14): 1884-1896.
- [18] An Z S, Clemens S C, Shen J et al. Glacial-interglacial Indian summer monsoon dynamics [J]. *Science*, 2011, 333(6043): 719-723.
- [19] Hao Q Z, Wang L, Oldfield F et al. Delayed build-up of Arctic ice sheets during 400, 000-year minima in insolation variability [J]. *Nature*, 2012, 490(7420): 393-396.
- [20] Lu H Y, Yi S W, Liu Z Y et al. Variation of East Asian monsoon precipitation during the past 21 k. y. and potential CO<sub>2</sub> forcing [J]. *Geology*, 2013, 41(9): 1023-1026.
- [21] Shi P H, Yang T B, Tian Q C et al. Loess record of climatic changes during MIS 12-10 in the Jingyuan section, northwestern Chinese Loess Plateau [J]. *Quaternary International*, 2013, 296: 149-159.
- [22] Song Y G, Fang X M, King J W et al. Magnetic parameter variations in the Chaona loess/paleosol sequences in the central Chinese Loess Plateau, and their significance for the middle Pleistocene climate transition [J]. *Quaternary Research*, 2014, 81(3): 433-444.
- [23] Kang S G, Wang X L, Roberts H M et al. Late Holocene anti-phase change in the East Asian summer and winter monsoons [J]. *Quaternary Science Reviews*, 2018, 188: 28-36.
- [24] Liu J B, Shen Z W, Chen W et al. Dipolar mode of precipitation changes between north China and the Yangtze River Valley existed over the entire Holocene: Evidence from the sediment record of Nanyi Lake [J]. *International Journal of Climatology*, 2021, 41(3): 1667-1681.
- [25] 张月婷, 吴乃琴, 李丰江, 等. 低偏心率间冰期(Mis 19)黄土高原生态环境变化及影响机制[J]. *中国科学: 地球科学*, 2020, 63(9): 1408-1421. [ZHANG Yueting, WU Naiqin, LI Fengjiang et al. Eco-environmental changes in the Chinese Loess Plateau during low-eccentricity interglacial Marine Isotope Stage 19 [J]. *Science China Earth Sciences*, 2020, 63(9): 1408-1421.]
- [26] Wang Y J, Cheng H, Edwards R L et al. Millennial- and orbital-scale changes in the East Asian monsoon over the past 224, 000 years [J]. *Nature*, 2008, 451(7182): 1090-1093.
- [27] Cheng H, Edwards R L, Sinha A et al. The Asian monsoon over the past 640, 000 years and ice age terminations [J]. *Nature*, 2016, 534(7609): 640-646.
- [28] Chen F H, Yu Z C, Yang M L et al. Holocene moisture evolution in arid central Asia and its out-of-phase relationship with Asian monsoon history [J]. *Quaternary Science Reviews*, 2008, 27(3-4): 351-364.
- [29] Zhao Y, Tzedakis P C, Li Q et al. Evolution of vegetation and climate variability on the Tibetan Plateau over the past 1.74 million years [J]. *Science Advances*, 2020, 6(19): eaay6193.
- [30] Lisiecki L E, Raymo M E. A Pliocene-Pleistocene stack of 57 globally distributed benthic δ<sup>18</sup>O records [J]. *Paleoceanography*, 2005, 20(1): PA1003.
- [31] Wang P X, Wang B, Cheng H et al. The global monsoon across timescales: coherent variability of regional monsoons [J]. *Climate of the Past*, 2014, 10(6): 2007-2052.
- [32] Nomade S, Bassinot F, Marino M et al. High-resolution foraminifer stable isotope record of MIS 19 at Montalbano Jonico, southern Italy: a window into Mediterranean climatic variability during a low-eccentricity interglacial [J]. *Quaternary Science Reviews*, 2019, 205: 106-125.
- [33] Huang E Q, Tian J, Steinke S. Millennial-scale dynamics of the winter cold tongue in the southern South China Sea over the past 26 ka and the East Asian winter monsoon [J]. *Quaternary Research*, 2011, 75(1): 196-204.
- [34] Loutre M F, Berger A. Marine isotope stage 11 as an analogue for the present interglacial [J]. *Global and Planetary Change*, 2003, 36(3): 209-217.
- [35] Ding Z L, Liu T, Rutter N W et al. Ice-volume forcing of East Asian winter monsoon variations in the past 800, 000 years [J]. *Quaternary Research*, 1995, 44(2): 149-159.
- [36] Liu T, Ding Z L. Chinese loess and the paleomonsoon [J]. *Annual Review of Earth and Planetary Sciences*, 1998, 26: 111-145.
- [37] Sun Y B, Kutzbach J, An Z S et al. Astronomical and glacial forcing of East Asian summer monsoon variability [J]. *Quaternary Science Reviews*, 2015, 115: 132-142.
- [38] Wu C H, Tsai P C. Obliquity-driven changes in East Asian seasonality [J]. *Global and Planetary Change*, 2020, 189: 103161.
- [39] Roychowdhury R. Eccentricity Modulation of Precessional Variation in the Earth's Climate Response to Astronomical Forcing: a Solution to the 41-kyr Mystery[D]. Doctor dissertation, University of Massachusetts Amherst, 2018.
- [40] 石正国, 雷婧, 周朋, 等. 轨道尺度亚洲气候演化机理的数值模拟: 历史与展望[J]. *第四纪研究*, 2020, 40(1): 8-17. [SHI Zhengguo, LEI Jing, ZHOU Peng et al. Numerical simulation researches on orbital-scale Asian climate dynamics: history and perspective [J]. *Quaternary Sciences*, 2020, 40(1): 8-17.]
- [41] Wang Z X, Huang C J, Licht A et al. Middle to late Miocene eccentricity forcing on lake expansion in NE Tibet [J]. *Geophysical Research Letters*, 2019, 46(12): 6926-6935.
- [42] Nie J S, Garzione C, Su Q D et al. Dominant 100, 000-year precipitation cyclicity in a late Miocene lake from northeast Tibet [J]. *Science Advances*, 2017, 3(3): e1600762.
- [43] Wang Z X, Shen Y J, Licht A et al. Cyclostratigraphy and magnetostratigraphy of the middle Miocene Ashigong Formation, Guide Basin, China, and its implications for the paleoclimatic evolution of NE Tibet [J]. *Paleoceanography and Paleoclimatology*, 2018, 33(10): 1066-1085.
- [44] Han W X, Appel E, Galy A et al. Climate transition in the Asia inland at 0.8-0.6 Ma related to astronomically forced ice sheet expansion [J]. *Quaternary Science Reviews*, 2020, 248: 106580.
- [45] Miao Y F, Fang X M, Herrmann M et al. Miocene pollen record of KC-1 core in the Qaidam Basin, NE Tibetan Plateau and implications for evolution of the East Asian monsoon [J]. *Palaeogeography, Palaeoclimatology, Palaeoecology*, 2011, 299(1-2): 30-38.
- [46] Zhuang G S, Hourigan J K, Koch P L et al. Isotopic constraints on intensified aridity in Central Asia around 12Ma [J]. *Earth and Planetary Science Letters*, 2011, 312(1-2): 152-163.
- [47] Fang X M, Zhang W L, Meng Q Q et al. High-resolution magneto-

- stratigraphy of the Neogene Huaitoutala section in the eastern Qaidam Basin on the NE Tibetan Plateau, Qinghai Province, China and its implication on tectonic uplift of the NE Tibetan Plateau [J]. *Earth and Planetary Science Letters*, 2007, 258(1-2): 293-306.
- [48] Lu H J, Xiong S F. Magnetostratigraphy of the Dahonggou section, northern Qaidam Basin and its bearing on Cenozoic tectonic evolution of the Qilian Shan and Altyn Tagh Fault [J]. *Earth and Planetary Science Letters*, 2009, 288(3-4): 539-550.
- [49] Chang H, Li L Y, Qiang X K et al. Magnetostratigraphy of Cenozoic deposits in the western Qaidam Basin and its implication for the surface uplift of the northeastern margin of the Tibetan Plateau [J]. *Earth and Planetary Science Letters*, 2015, 430: 271-283.
- [50] Ji J L, Zhang K X, Clift P D et al. High-resolution magnetostratigraphic study of the Paleogene-Neogene strata in the Northern Qaidam Basin: implications for the growth of the Northeastern Tibetan Plateau [J]. *Gondwana Research*, 2017, 46: 141-155.
- [51] Wang W T, Zheng W J, Zhang P Z et al. Expansion of the Tibetan Plateau during the Neogene [J]. *Nature Communications*, 2017, 8(1): 15887.
- [52] Nie J S, Ren X P, Saylor J E et al. Magnetic polarity stratigraphy, provenance, and paleoclimate analysis of Cenozoic strata in the Qaidam Basin, NE Tibetan Plateau [J]. *GSA Bulletin*, 2020, 132(1-2): 310-320.
- [53] Chen F H, Jia J, Chen J H et al. A persistent Holocene wetting trend in arid central Asia, with wettest conditions in the late Holocene, revealed by multi-proxy analyses of loess-paleosol sequences in Xinjiang, China [J]. *Quaternary Science Reviews*, 2016, 146: 134-146.
- [54] 汤良杰, 金之钧, 戴俊生, 等. 柴达木盆地及相邻造山带区域断裂系统 [J]. 地球科学——中国地质大学学报, 2002, 27(6): 676-682. [TANG Liangjie, JIN Zhijun, DAI Junsheng et al. Regional fault systems of Qaidam Basin and adjacent Orogenic belts [J]. *Earth Science-Journal of China University of Geosciences*, 2002, 27(6): 676-682.]
- [55] Bush M A, Saylor J E, Horton B K et al. Growth of the Qaidam Basin during Cenozoic exhumation in the northern Tibetan Plateau: inferences from depositional patterns and multiproxy detrital provenance signatures [J]. *Lithosphere*, 2016, 8(1): 58-82.
- [56] 刘青松, 邓成龙. 磁化率及其环境意义 [J]. *地球物理学报*, 2009, 52(4): 1041-1048. [LIU Qingsong, DENG Chenglong. Magnetic susceptibility and its environmental significances [J]. *Chinese Journal of Geophysics*, 2009, 52(4): 1041-1048.]
- [57] Liu Q S, Jackson M J, Banerjee S K et al. Mechanism of the magnetic susceptibility enhancements of the Chinese loess [J]. *Journal of Geophysical Research: Solid Earth*, 2004, 109(B12): B12107.
- [58] Maher B A, Thompson R. Paleorainfall reconstructions from pedogenic magnetic susceptibility variations in the Chinese loess and paleosols [J]. *Quaternary Research*, 1995, 44(3): 383-391.
- [59] Nie J S, Song Y G, King J W et al. Consistent grain size distribution of pedogenic maghemite of surface soils and Miocene loessic soils on the Chinese Loess Plateau [J]. *Journal of Quaternary Science*, 2010, 25(3): 261-266.
- [60] Song Y, Hao Q Z, Ge J Y et al. Quantitative relationships between magnetic enhancement of modern soils and climatic variables over the Chinese Loess Plateau [J]. *Quaternary International*, 2014, 334-335: 119-131.
- [61] Holbourn A, Kuhnt W, Clemens S et al. Middle to late Miocene stepwise climate cooling: evidence from a high-resolution deep water isotope curve spanning 8 million years [J]. *Paleoceanography*, 2013, 28(4): 688-699.
- [62] Holbourn A, Kuhnt W, Clemens S C et al. A ~12 Myr Miocene record of east Asian monsoon variability from the South China Sea [J]. *Paleoceanography and Paleoclimatology*, 2021, 36(7): e2021PA004267.
- [63] Li T, Liu F, Abels H A et al. Continued obliquity pacing of East Asian summer precipitation after the mid-Pleistocene transition [J]. *Earth and Planetary Science Letters*, 2017, 457: 181-190.
- [64] Mantysis D F, Lintner B R, Broccoli A J et al. The response of large-scale circulation to obliquity-induced changes in meridional heating gradients [J]. *Journal of Climate*, 2014, 27(14): 5504-5516.
- [65] Levy R H, Meyers S R, Naish T R et al. Antarctic ice-sheet sensitivity to obliquity forcing enhanced through ocean connections [J]. *Nature Geoscience*, 2019, 12(2): 132-137.
- [66] Ao H, Roberts A P, Dekkers M J et al. Late Miocene–Pliocene Asian monsoon intensification linked to Antarctic ice-sheet growth [J]. *Earth and Planetary Science Letters*, 2016, 444: 75-87.
- [67] Mantysis D F, Clement A C, Broccoli A J et al. Climate feedbacks in response to changes in obliquity [J]. *Journal of Climate*, 2011, 24(11): 2830-2845.
- [68] Chen G S, Liu Z Y, Clemens S C et al. Modeling the time-dependent response of the Asian summer monsoon to obliquity forcing in a coupled GCM: a PHASEMAP sensitivity experiment [J]. *Climate Dynamics*, 2011, 36(3): 695-710.
- [69] Ren X P, Nie J S, Saylor J E et al. Provenance control on chemical weathering index of Fluvio-Lacustrine sediments: evidence from the Qaidam Basin, NE Tibetan Plateau [J]. *Geochemistry, Geophysics, Geosystems*, 2019, 20(7): 3216-3224.